International Psychogeriatrics (2011), Vol. 23, Supplement 2, S13–S24 © International Psychogeriatric Association 2011
doi:10.1017/S1041610211000913

Structural MRI

Mike P. Wattjes

Alzheimer Center Amsterdam, Department of Radiology, VU University Medical Center, Amsterdam, The Netherlands

ABSTRACT

Clinical neuroimaging is increasingly being used in the diagnosis of neurodegenerative diseases and has become one of the most important paraclinical tools in the diagnosis of dementia. According to current guidelines, neuroimaging, preferably magnetic resonance imaging (MRI), should be performed at least once during the diagnostic work-up of patients with suspected or definite dementia. MRI is helpful in identifying or excluding potentially treatable causes of dementia; however, these account only for a small proportion of dementias. In addition, MRI is able to support the clinical diagnosis in a memory clinic setting by identifying certain patterns of atrophy and vascular damage. Visual rating scales are well-established methods in the clinical routine for the assessment and quantification of regional/global cortical atrophy, hippocampal atrophy and vascular damage. In addition, MRI is able to detect certain aspects of pathology associated with dementia, such as cerebral microbleeds which are related to cerebral amyloid angiopathy and Alzheimer pathology. This review paper aims to give an overview of the application of structural MRI in the diagnostic procedure for memory clinic patients in terms of excluding and supporting the diagnosis of various diseases associated with dementia.

Key words: dementia, neuroimaging, magnetic resonance imaging, Alzheimer's disease

Introduction

Clinical neuroimaging is increasingly being used in the diagnostic work-up of patients presenting to a memory clinic. Structural neuroimaging methods such as computed tomography (CT) and, more sensitively, magnetic resonance imaging (MRI) are well suited to exclude possibly (surgically) treatable cause of dementia (e.g. tumors, subdural hematomas, hydrocephalus, etc.). However, these patients represent the vast minority (<8%) of patients presenting with memory complaints to a memory clinic (Scheltens *et al.*, 2002). More importantly, structural brain imaging can demonstrate certain patterns of atrophy, vascular pathology or inflammatory changes, which can substantially support the clinical diagnosis of dementia. In other words, during the past decade, the role of structural neuroimaging as a diagnostic tool in a memory clinic setting has changed from an exclusionary to a more inclusionary approach. In addition, MRI is increasingly being used for disease monitoring (e.g. progression of atrophy and vascular changes) and has therefore been established as a valuable method for efficacy and safety monitoring in clinical treatment trials (Frisoni *et al.*, 2010). As a consequence, this has led to the incorporation of clinical neuroimaging into current diagnostic guidelines of dementia, which state that neuroimaging should be performed at least once during the diagnostic work-up of patients with suspected or definite dementia (Hort *et al.*, 2010).

Correspondence should be addressed to: Mike P. Wattjes, MD, Alzheimer Center Amsterdam, Department of Radiology, VU University Medical Center, De Boelelaan 1117, 1081 HV Amsterdam, The Netherlands. Phone: +31 20-444-0341; Fax: +31 20-444-0397. Email: m.wattjes@vumc.nl. First published online 10 June 2011.

Structural MRI protocol in dementia

Multidetector CT is a suitable diagnostic method for the exclusion of possible treatable causes of dementia, as well as for the assessment and visual rating of focal and global cortical atrophy, atrophy of the medial temporal lobe and vascular white matter changes (Wattjes *et al.*, 2009). However, structural MRI is the imaging modality of choice due to the lack of radiation, better gray matter/ white matter contrast, and the ability to manipulate tissue contrast with different pulse sequences.

The MRI protocol should include pulse sequences which address the following issues: assessment of focal and global cortical atrophy as well as atrophy of the medial temporal lobe (particularly the hippocampus); vascular white

Table 1. Example of a multisequence MRI protocol for patients presenting to a memory clinic

3D-T1 with MPR	Assessment of the medial temporal lobe on oblique coronal reconstructions according to the axis of the hippocampus
Axial FLAIR (preferably 3D dataset)	Assessment of vascular white matter changes, global and focal cortical atrophy
Axial T2-(T)SE	Assessment of vascular changes in deep gray matter structures (e.g. lacunar infarctions of the thalamus)
Axial T2*-GE	Detection of microbleeds and macrohemorrhages
Axial DWI	Detection of areas with restricted diffusion (e.g. acute stroke, Creutzfeld–Jakob disease, Herpes encephalitis)

D = dimensional; DWI = diffusion-weighted imaging; FLAIR = fluid-attenuated inversion recovery; MPR = multiplanar reconstructions; TSE = turbo spin echo; GE = gradient echo.

Table 2. Overview of the most established visual rating scales for the assessment of cortical atrophy, hippocampal atrophy (medial temporal lobe atrophy, MTA) and white matter hyperintensities (WMH)

	CORTICAL ATROPHY PASQUIER SCALE	MTA SCHELTENS SCALE	WMH FAZEKAS SCALE
Grade 0	Normal	Normal	No lesions
Grade 1	Widened sulci	↑ Width choroid fissure	Punctiforme lesions
Grade 2	Widened sulci Volume loss of the gyri	↑ Width of the choroid fissure ↑ Width of the temporal horn	Partially confluent lesions
Grade 3	Knife blade atrophy	↑↑ Width of the choroid fissure ↑↑ Width of the temporal horn ↑ Volume loss hippocampus	Confluent lesions
Grade 4	–	↑↑↑ Width of the choroid fissure ↑↑ Width of the temporal horn ↑↑ Volume loss hippocampus	–

matter changes (small and large vessel disease); vascular changes in deep gray matter structures (in particular thalamus infarction); cerebral microbleeds (MBs) and macrohemorrhages (including post-traumatic changes). An example of a possible MRI multisequence protocol is given in Table 1.

How to read MRI scans in memory clinic patients

MRI scans in a clinical routine setting should be read in a structured and reproducible way. Regarding the two most relevant pathological features in dementia (cortical atrophy including medial temporal lobe atrophy and vascular changes), visual rating scales have been established, validated and are widely used in a clinical routine setting. Table 2 summarizes the most established rating scales for focal and global cortical atrophy, hippocampal atrophy and vascular white matter changes. In addition, certain aspects of MRI pathology associated with cognition and normal aging, such as the presence of MBs, should be assessed and classified.

Cortical atrophy

Visual rating of cortical atrophy can be easily performed using the four-point (0–3) Pasquier scale (Pasquier *et al.*, 1996) based on the width of the sulci and volume of the gyri (Figure 1). The Pasquier scale can be applied either globally (global cortical atrophy) or regionally for certain anatomic regions (temporal, parietal, etc.).

Medial temporal lobe atrophy

The visual rating of medial temporal lobe atrophy is more sophisticated since we are dealing with a complex interaction of rather small anatomic structures and landmarks. The five-point Scheltens scale, considering the width of the choroid fissure, temporal horn as well as the volume of the hippocampus, is a well-established rating scale for the assessment of the medial temporal lobe, which correlates well with histopathology and volumetric measurements (Scheltens *et al.*, 1992) (Figure 1).

Vascular pathology

The assessment of vascular changes is crucial in the radiological evaluation of dementia patients,

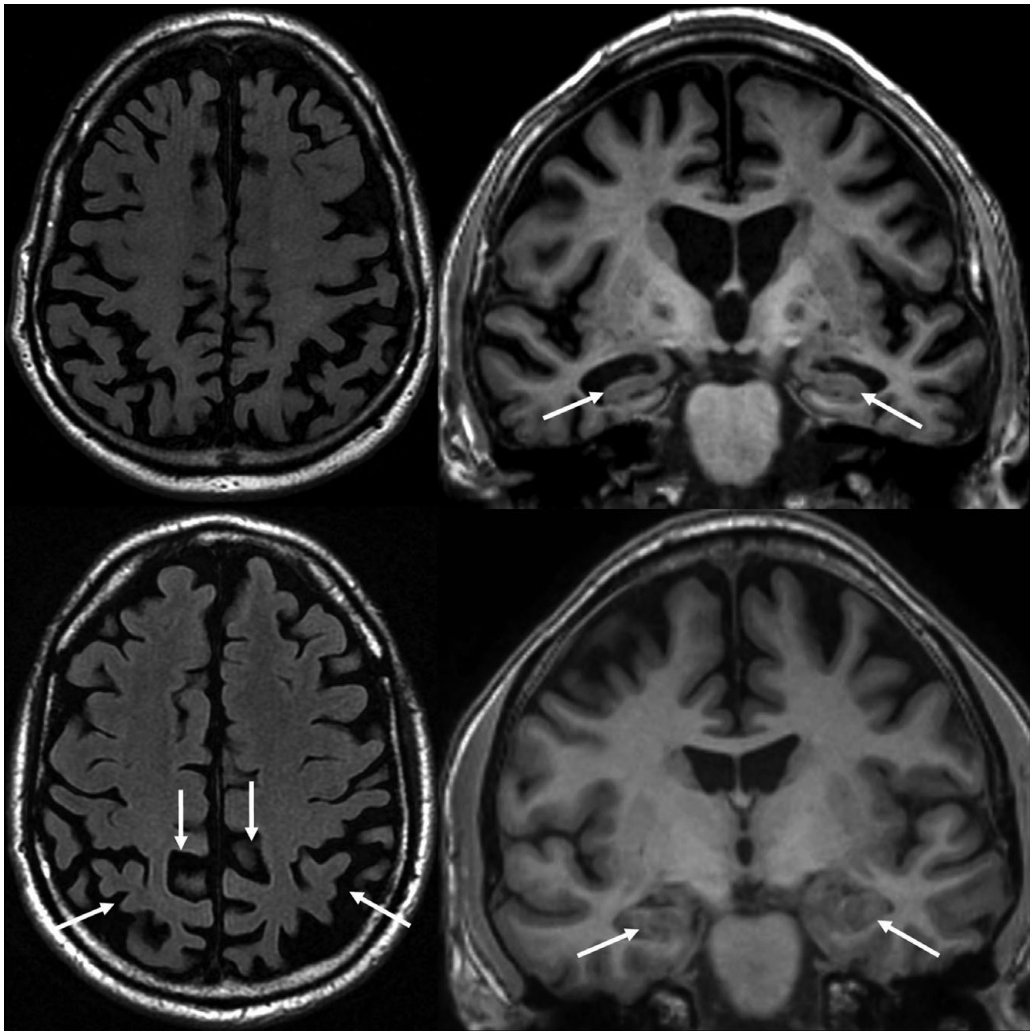

Figure 1. MRI findings in patients presenting with Alzheimer's disease (AD). Top row: axial FLAIR (left) and oblique coronal reconstructions (according to the axis of the hippocampus) of a 3D T1-weighted sequence (right) obtained from an 81-year-old male presenting with a late-onset (senile) type of AD. On the FLAIR images, a severe global cortical atrophy (grade 2) can be observed. The cortical atrophy is more prominent but not restricted to the parietal lobes. In addition, substantial (grade 2) atrophy of the hippocampus (widening of the choroid fissure in combination with a volume loss of the hippocampus) is present (arrows). Bottom row: comparable MR images obtained from a 50-year-old male presenting with an early-onset (presenile) type of AD. In these patients a rather focal atrophy pattern involving the parietal lobe (left, arrows), including the precuneus and the posterior cingulate, can be frequently observed, while the medial temporal lobe structures are relatively spared (right, arrows).

particularly for the diagnosis of vascular dementia (VaD) (van Straaten *et al.*, 2004). However, small vessel white matter changes which do not formally fulfill the diagnostic criteria for VaD act in a synergistic way with neurodegenerative changes with relevant impact on clinical outcome measures (Inzitari *et al.*, 2009). FLAIR is the most sensitive MRI sequence for the detection of white matter hyperintensities (WMH) as a marker of small vessel vascular damage. An easily applicable and highly reproducible four-point rating scale (Fazekas scale) is widely used in clinical practice and corresponds well with more detailed ratings scales and histopathology (Fazekas *et al.*, 1987, Scheltens *et al.*, 1998). Another important marker of small vessel disease, which has been included into the NINDS-AIREN criteria for VaD, is the presence of lacunar infarcts (Román *et al.*, 1993). These are strongly associated with the presence and amount of WMH and can be frequently found in the cerebral deep white matter, basal ganglia and crucial anatomic structures such as the thalamus. Lacunes in the white matter can also be sensitively detected and differentiated from perivascular spaces on FLAIR sequences (Figure 2). However, lacunes in the infratentorial white matter and deep gray matter structures (particularly the thalamus) are frequently missed on FLAIR and therefore T2-weighted (turbo) spin-echo sequences are mandatory for these purposes (Bastos-Leite *et al.*, 2004).

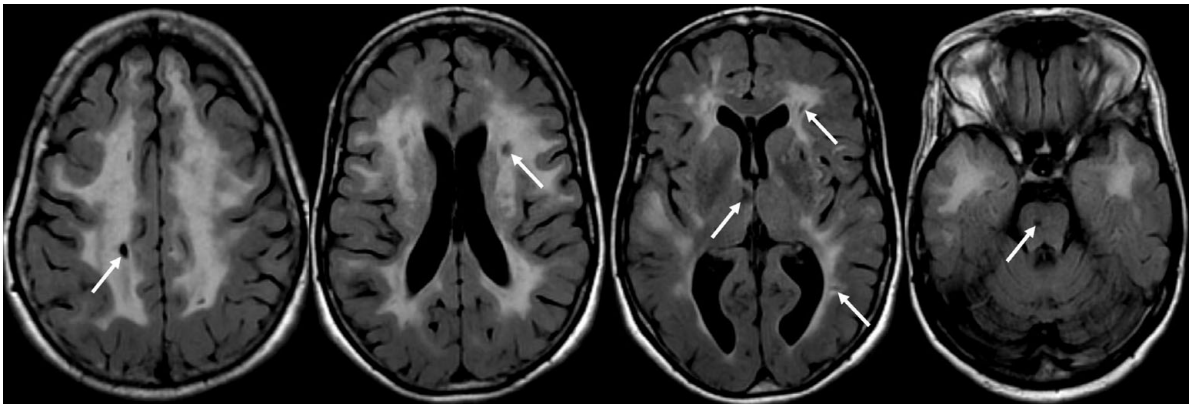

Figure 2. Axial FLAIR images obtained from a 47-year-old female diagnosed with vascular dementia according to the NINDS-AIREN criteria. On MRI, confluent WMH (Fazakas grade 3) can be observed involving more than 25% of the white matter. Multiple lacunes (arrows) are present in the deep white matter but also in the basal ganglia region. Note the severe involvement of the white matter of the anterior temporal lobe suggestive of CADASIL (cerebral autosomal dominant arteriopathy with subcortical infarcts and leukoencephalopathy). In fact, a mutation in the Notch-3 gene was found in this patient.

Besides the assessment of small vessel disease, the detection of large vessel disease, including territorial infracts and watershed infarcts are of importance since they have been incorporated into the NINDS-AIREN criteria for VaD (Román *et al.*, 1993).

Cerebral microbleeds

MBs are defined as small hypointense dot-like lesions in the brain parenchyma on T2*-weighted or susceptibility weighted MRI (SWI). Pathologically, MBs represent perivascular hemosiderin deposits stored in surrounding macrophages, presumably due to pathological amyloid deposition in the vascular wall leading to permeability and leakage. Alternatively, MBs can also be seen in association with small vessel disease, i.e. with hyperintense vasculopathy. In terms of anatomic distribution and the underlying pathophysiology, MBs can be subdivided in lobar MBs located in the cortical gray–white matter interface and non-lobar MBs located in deep brain structures (e.g. basal ganglia) and the posterior fossa (Figure 3). Lobar MBs are related to cerebral amyloid angiopathy (CAA), and almost invariably present in patients with Alzheimer's disease (AD), whereas non-lobar MBs are more related to hypertensive vasculopathy (Cordonnier and van der Flier, 2011). These two different vasculopathies may co-occur in dementia patients.

Depending on the sensitivity of the imaging technique (magnetic field strengths, pulse sequences, echo time, spatial resolution), the prevalence of MB in a normal elderly healthy population is almost 25% (Poels *et al.*, 2011). In a memory clinic population, the prevalence of MB is approximately 17%, ranging from 10% in patients with subjective memory complaints, 18–20% in AD, to 65% in patients with VaD (Cordonnier *et al.*, 2006). In general, MBs are associated with clinical outcome measures, such as cognitive function and mortality, age, apolipoprotein E genotype, cerebrospinal fluid biomarkers, as well as vascular damage seen on MRI, including WMH and lacunes (Goos *et al.*, 2009; 2010). In addition, there is emerging evidence that lobar cortical MBs might have predictive value in terms of the future development of AD (Kirsch *et al.*, 2009). It is also conceivable that non-lobar MB might be a predictive factor of VaD, but this remains to be investigated.

Amyloid-associated leakage from leptomeningeal vessel leads to the pathological hemosiderin deposition in the subpial space, which has coined the term of superficial siderosis. On T2*-weighted and susceptibility-weighted MRI, superficial siderosis can be identified by low signal abnormalities in the subpial space lining the surface of the brain. Similar to lobar hemorrhage and MBs, superficial siderosis seems to be a marker for CAA (Linn *et al.*, 2010) (Figure 3). Its prevalence is rather lower than 1% among a normal healthy population and there is strong co-incidence with lobar MBs (Vernooij *et al.*, 2009). However, compared to MBs, the clinical and prognostic role of superficial siderosis in dementia patients is rather unclear and needs further investigation.

Use of MRI to support the diagnosis of neurological disease associated with dementia

Beside the assessment of normal aging findings (mild global cortical and hippocampal atrophy and WMH), MRI is helpful to support the clinical diagnosis of neurodegenerative, inflammatory and metabolic disease associated with dementia, by

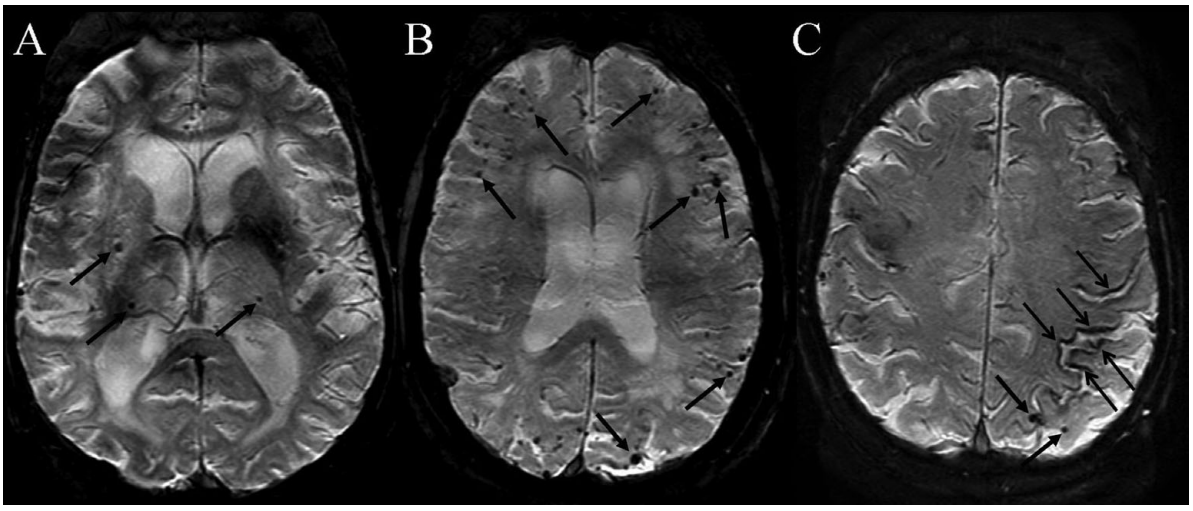

Figure 3. Axial SWI images presenting different types of microbleeds (MBs). (A) MBs (arrows) located in the deep white and gray matter structures (non-lobar) are associated with hypertensive encephalopathy whereas (B) MBs (arrows) located in the white matter–cortcial gray matter interface are rather associated with cerebral amyloid angiopathy (CAA). (C) Superficial siderosis (open head arrows) represents a leptomeningeal manifestation of CAA. In this patient, lobar MBs (closed head arrows) are located close to the areas of superficial siderosis.

showing specific atrophy patterns and white and/or gray matter changes. Here we describe the MRI pathology of the most frequent diseases associated with dementia.

Alzheimer's disease

AD is the most common cause of dementia and is characterized by the histopathological hallmarks of amyloid-β and hyperphophorylated tau accumulation (McKhann *et al.*, 1984). The role of neuroimaging in the diagnosis of AD is becoming increasingly important. This is reflected in new proposed diagnostic criteria in which, as well as cerebrospinal fluid (CSF) (amyloid-β_{42}, tau or phospho-tau) and positron emission tomography (PET) findings (temporo-parietal hypometabolism on FDG-PET, amyloid imaging), a structural imaging marker (medial temporal lobe atrophy) has been included as a key criterion for the diagnosis of AD (Dubois *et al.*, 2007).

Corresponding to the neuropathological stages described by Braak and Braak (1991), the neurodegenerative changes in terms of atrophy in senile AD patients can be detected first in the medial temporal lobe, particularly in the hippocampus and best seen on oblique coronal T1-weighted images. Although MTA is very characteristic for AD, a normal volume of the medial temporal lobe does not exclude AD. In addition, MTA is a common feature in other neurodegenerative disorders and is therefore not a specific marker to confidently exclude other neurodegenerative disease associated with dementia. Besides the diagnostic hallmark MTA, cortical atrophy predominantly located in the parietal lobes is a common radiological feature and may be helpful in differentiating AD from other neurodegenerative diseases associated with dementia (Jones *et al.*, 2006; Frisoni *et al.*, 2007) (Figure 1). The degree of cortical atrophy and MTA can be easily assessed by visual rating, as described above, and corresponds well with histopathology. Visual rating of MTA in a memory clinic population in order to distinguish AD patients from those without cognitive complaints provides sensitivity and specificity values of 80–85% (Frisoni *et al.*, 2010).

Compared to classical senile AD manifestations, early-onset (pre-senile) AD may present with a different distinct atrophy pattern predominantly involving the parietal cortex, precuneus and posterior cingulum and relatively sparing the medial temporal lobe (Figure 1). In advanced stages, the medial temporal lobe becomes more and more affected (Karas *et al.*; 2007; Shiino *et al.*, 2008).

In patients with mild cognitive impairment (MCI) who present with cognitive impairment not fulfilling the diagnostic criteria for dementia, the degree of cortical and hippocampal atrophy measured by visual rating has a strong predictive value for further cognitive decline and development of AD (Likeman *et al.*, 2005; Bouwman *et al.*, 2007; Davatzikos *et al.*; 2010).

It is important to realize that the vast majority of patients with AD pathology present with a combination of neurodegenerative changes and vascular pathology, such as WMH and lacunar infarcts. This vascular co-morbidity has prompted

the pathophysiological concept that AD patients do not usually present with a "pure Alzheimer pathology," which has coined the term of "mixed pathology" (de la Torre, 2004; DeCarli, 2006). This concept is further supported by the distribution of MBs in AD patients. The vast majority of MBs is located in lobar regions in the cortical white–gray matter interface, suggesting CAA pathology which is strongly associated with AD. However, a substantial proportion of MBs is located in non-lobar regions, suggesting underlying microangiopathy due to vasculo-ischemic damage. In fact, these findings further support the concept of "mixed pathology" and the clinical impression that amyloid pathology and cerebrovascular pathology are likely acting in a synergistic way (Kalaria and Ballard, 1999).

Fronto-temporal lobe degeneration

The disease entity of fronto-temporal lobe degeneration (FTLD) consists of three different and distinct clinical subtypes: the behavioral variant of fronto-temporal dementia (bvFTD), progressive aphasia (PA) and semantic dementia (SD). These subtypes present with different clinical manifestations and also different atrophy patterns on MRI (Neary *et al.*, 1998). The bvFTD is radiologically characterized by (bilateral) atrophy of the frontal lobes, including the dorsolateral, frontobasal and mesofrontal cortical areas, as well as of the anterior parts of the temporal lobes (Figure 4). PA is a non-fluent aphasia characterized by left-sided (most often) atrophy of the lateral parts of the temporal lobe, basal parts of the frontal lobe and the insular cortex, resulting in a unilateral widening of the Silvian fissure (Gorno-Tempini *et al.*, 2011). Semantic aphasia is a progressive form of fluent-aphasia and shows focal cortical atrophy of the anterior parts of the temporal lobes (temporal pole), more frequently on the left side than on the right side (Figure 4). These atrophy patterns correlate well with quantitative MRI methods, such as voxel-based morphometry (VBM), and with pathological studies.

In early disease stages, structural neuroimaging can be normal and/or shows unspecific global cortical atrophy, as seen in other dementias. In these stages, PET imaging may already reveal relevant glucose hypometabolism in fronto-temporal regions. The focal cortical atrophy pattern may develop slightly over time and become more evident in later disease stages. Also, medial temporal lobe structures such as the hippocampus and the amygdala are frequently affected. In patients with end-stage atrophy, a "ballooning" of the temporal horn can be observed, which is surrounded by a small confluent area of high signal in the white matter on T2-weighted images (Rosen *et al.*, 2002; Vitali *et al.*, 2008) (Figure 4).

Dementia associated with parkinsonian dementias

Most of the parkinsonian syndromes are associated with cognitive decline and dementia, including idiopathic Parkinson's disease, dementia with Lewy bodies (DLB), multisystem atrophy (MSA), corticobasal degeneration (CBD) and progressive supranuclear palsy (PSP).

Dementia with Lewy bodies

DLB is a frequent neurodegenerative disease associated with dementia, which is pathologically characterized by α-synuclein-positive Lewy body inclusions in the cortical gray matter. Clinically, DLB patients present with progressive cognitive impairment mainly affecting memory as well as visuo-spatial and executive domains, with fluctuations of symptoms combined with visual hallucinations and often sleeping disorders. Structural neuroimaging has limited value in the diagnosis of DLB. Most patients show mild to moderate global cortical atrophy, while the medial temporal lobe is relatively preserved (Figure 5). However, considering this atrophy pattern, there is substantial overlap between DLB and AD as well as normal aging. This overlap can be overcome by more specific imaging techniques, such as molecular imaging of the dopaminergic system (e.g. dopamine transporter imaging, DAT), allowing a more specific diagnosis of DLB.

Multisystem atrophy

Clinical characteristics of MSA include orthostatic hypotension, urine incontinence, and cerebellar symptoms. Imaging criteria of MSA consist of focal atrophy of the basal ganglia, in particular of the putamen, as well as the cerebellar peduncles (most obvious in the middle cerebellar peduncle), brain stem and cerebellum. On T2-weighted images of some MSA patients, linear signal abnormalities can be observed in white matter lateral to the putamen ("putaminal rim sign"), pons ("hot cross bun sign") and cerebellar peduncles, which can further support the clinical diagnosis of MSA (Figure 6) (Vitali *et al.*, 2008).

Cortical degeneration

Patients with CBD typically present with asymmetric cortical symptoms, including language and speech disturbances, visuo-spatial deficits and hemineglect, apraxia and occasionally myclonus, together with extra pyramidal signs. On MRI, CBD

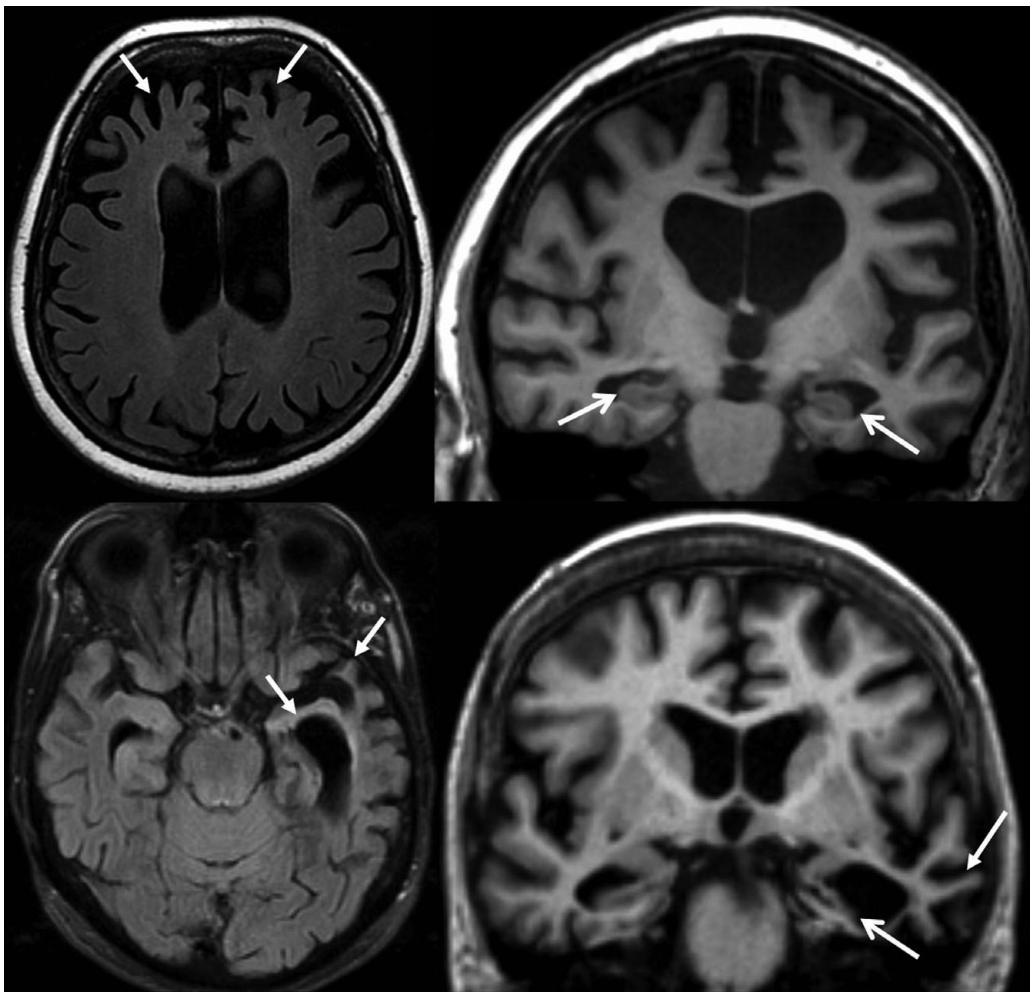

Figure 4. Axial FLAIR (left column) and oblique coronal reconstruction of a 3D T1-weighted sequence (right column) presenting different types of fronto-temporal lobe degeneration (FTLD). Top row: a 56-year-old female presenting with bvFTD. Note the focal atrophy of the frontal lobes (particularly of the mesofrontal area) (arrows). Atrophy of the medial temporal lobe structures (open head arrows) can also be observed in these patients and definitely does not exclude FTLD. Bottom row: a 76-year-old female presenting with semantic dementia. On MRI, a severe focal and asymmetric atrophy of the left temporal lobe can be observed in the vast majority of cases (open head arrows). In particular the temporal pole is affected. Ballooning of the temporal horn and a small rim of high signal on the FLAIR/T2-weighted images can be seen around the temporal horn, which is probably a gliotic reaction as a consequence of end-stage atrophy (arrows).

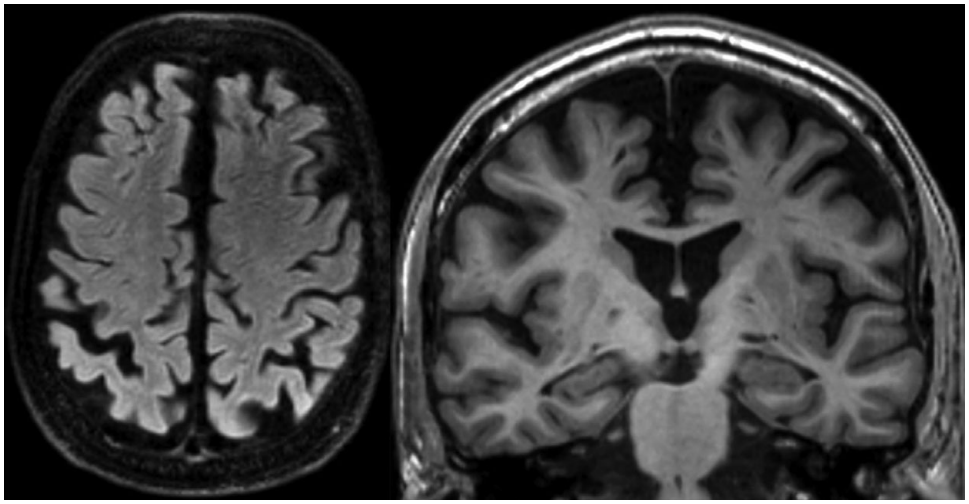

Figure 5. Axial FLAIR (left) and oblique coronal reconstruction of a 3D T1-weighted sequence (right) obtained from a 75-year-old male with DLB. Note the mild to moderate global cortical atrophy and the relative sparing of the hippocampus.

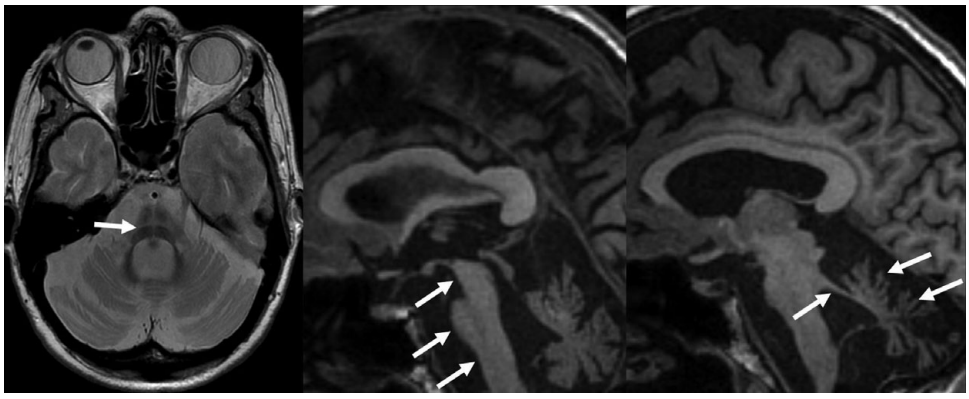

Figure 6. Axial T2-weighted (left) and sagittal T1-weighted MR images (middle and right) in a patient presenting with multisystem atrophy. Note the severe atrophy of the brain stem and the cerebellum, including the middle cerebellar peduncle (arrows). In the pons, two linear areas with high signal ("hot cross bun sign") can be detected on the T2-weighted image.

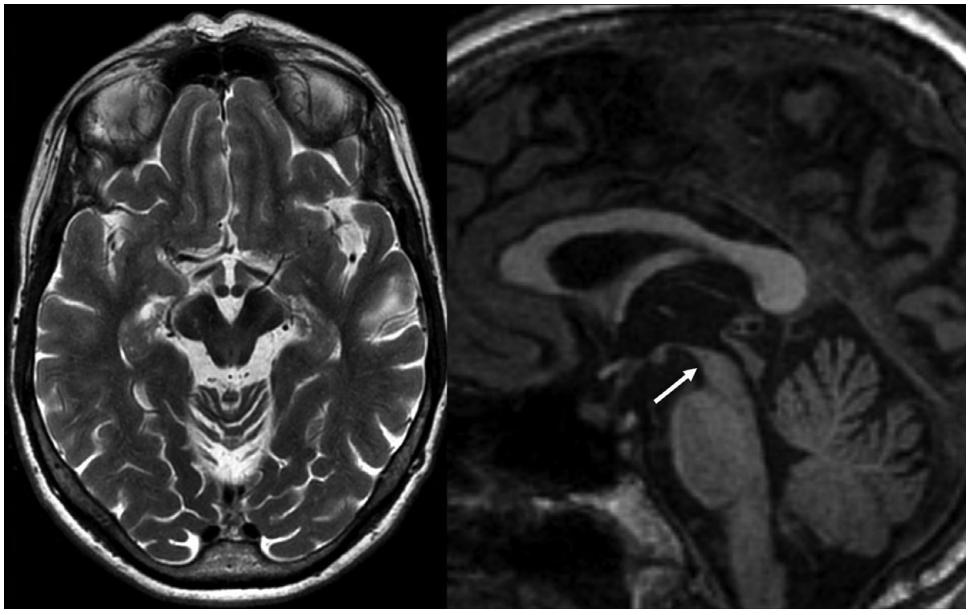

Figure 7. Axial T2-weighted and sagittal T1-weighted MR images of a patients with the diagnosis of progressive supranuclear palsy demonstrating mesencephalic atrophy (reduced gap diameter, increased interpeduncular angle), while the pons is relatively preserved. This atrophy pattern resembles the head and body of a humming bird, which has coined the term "humming bird" sign (arrow).

patients frequently show an asymmetric cortical atrophy of the parietal and frontal cortex,while the temporal lobe, including the medial temporal lobe, is relatively spared. The left side seems to be involved more frequently, and VBM analysis has shown that the neurodegenerative changes are most pronounced at the interface between the superior frontal and precentral sulci (Boxer *et al.*, 2006)

Progressive supranuclear palsy

PSP is clinically characterized by vertical eye movement disturbances and postural instability. MRI frequently shows indirect and direct evidence of mid-brain atrophy (Figure 7). An often used and reproducible MRI parameter is the anterior–posterior diameter of the mid-brain, which is significantly reduced in PSP patients. Different cut-off values of the anterior–posterior midbrain diameter have been reported. A diameter shorter than 15 mm measured in the mid-sagittal view has been well established and validated in a PSP population. In addition, a reduced volume of the cerebral peduncles and an increased inter-peduncular angle can be observed (Warmuth-Metz *et al.*, 2001; Oba *et al.*, 2005). However, mid-brain atrophy is a rather non-specific feature in the diagnosis of PSP since other neurodegenerative diseases, including CBD and MSA, can present with mid-brain atrophy, resulting in a considerable overlap. Studies also considering other key structures such as the middle and superior cerebellar peduncles were able to better differentiate PSP from MSA and Parkinson's disease.

Vascular dementia

Vascular dementia (VaD) is probably the most common cause of dementia after AD. Clinically, VaD is characterized by memory impairment and dysfunction of other cognitive domains, particularly frontal-executive functions. Neuroimaging plays a key role in the diagnosis of VaD. CT and, more sensitively, MRI are able to make the diagnosis of VaD according to diagnostic criteria and can distinguish pure VaD pathology from vascular comorbidity in terms of "mixed pathology." Within the group of VaD patients, the distinct pattern of distribution of vascular lesions can lead to a specific diagnosis of the underlying disease causing VaD, e.g. CADASIL (cerebral autosomal dominant arteriopathy with subcortical infarcts and leukoencephalopathy) (Chabriat *et al.*, 1998) (Figure 2).

Diagnostic criteria for VaD have been proposed with differing sensitivity and sensibility (Pohjasvaara *et al.*, 2000). The NINDS-AIREN criteria have been developed for establishing the diagnosis of VaD in research studies and clearly state that neuroimaging is an essential part of the diagnostic process of VaD. According to these criteria, patients can be classified as possible, probable and definite VaD. The NINDS-AIREN criteria are based on three main features: the presence of dementia, evidence of cerebro-vascular disease either clinically or in MRI/CT, and the temporal relationship between the clinical onset of dementia and the cerebrovascular disease. Radiologically, VaD can be diagnosed based on the presence of small vessel disease (WMH affecting at least 25% of the white matter, multiple basal ganglia and frontal white matter lacunes, bilateral thalamic lesions) and large vessel disease (territorial and watershed infarcts) (Guermazi *et al.*, 2007). Regarding the latter, both the severity (e.g. bilateral) and location (e.g. dominant hemisphere and involving association cortex) are crucial parameters. However, the diagnosis within strict diagnostic criteria remains a matter for debate. The temporal relationship between vascular damage (e.g. stroke) and cognitive decline is difficult to determine in many cases since a substantial number of strokes and, moreover, progression of WMH is silent. In addition, chronic hemodynamic conditions leading to cerebral hypoperfusion (e.g. carotid stenosis) may cause cognitive impairment and dementia without any vascular changes stated in the diagnostic criteria (Johnston *et al.*, 2004). Elderly patients with dementia who fulfill the clinico-radiological diagnostic criteria of VaD in particular also show changes consistent with AD pathology, which again reinforces the concept of "mixed dementia." Another possible limitation of VaD diagnostic criteria is that MBs, which are associated with cognitive deficits in several populations, are currently not being considered.

Despite the difficulties and problems in the diagnosis of VaD, neuroimaging has become crucial in identifying certain patterns of vascular damage causing VaD, as well as identifying underlying vascular pathology in the early disease course, which might have therapeutic consequences (Tzourio *et al.*, 2003).

Dementia secondary to inflammation

Besides primary neurodegenerative diseases associated with dementia, cognitive decline is commonly associated with neuroinflammatory and infectious disease of the central nervous system, including multiple sclerosis, herpes simplex infections, progressive multifocal leukoencephalopathy (PML) and prion diseases. Concerning the diagnosis of prion diseases such as Creutzfeld-Jakob disease (CJD), MRI has become one of the most important diagnostic methods. Depending on the clinical subtype of CJD, different patterns of high signal abnormalities on FLAIR and T2-weighted imaging can be observed in the cortical gray matter and the basal ganglia, particularly the striatum and thalamus (Figure 8). The abnormalities show features of restricted extracellular diffusion with a high signal on diffusion-weighted imaging and corresponding low apparent diffusion coefficient (ADC) values (Shiga *et al.*, 2004). Different patterns of gray matter involvement on MRI in sporadic (sCJD), genetic and variant (vCJD) forms of CJD have been described (Zeidler *et al.*, 2000; Tschampa *et al.*, 2007). Based on pattern recognition, MRI diagnosis of CJD can be made with a high sensitivity and specificity beyond 90%. Therefore, MRI may not only support the clinical diagnosis of CJD, but also allow a rather specific diagnosis of CJD in combination with other biomarkers, including the CSF (14–3-3 protein) and electroencephalogram.

Serial MRI

The atrophy patterns in neurodegenerative disease described above are based on cross-sectional MRI. In neurodegenerative diseases such as AD, the atrophy rate is more accelerated when compared to normal aging brains. Therefore, serial MRI examinations can assess atrophy progression during follow-up, which can further support the clinical diagnosis, particularly in early disease stages when the neurodegenerative findings might be rather discrete (Jack *et al.*, 1998; Riidha *et al.*, 2006). With the advent of more specific imaging methods

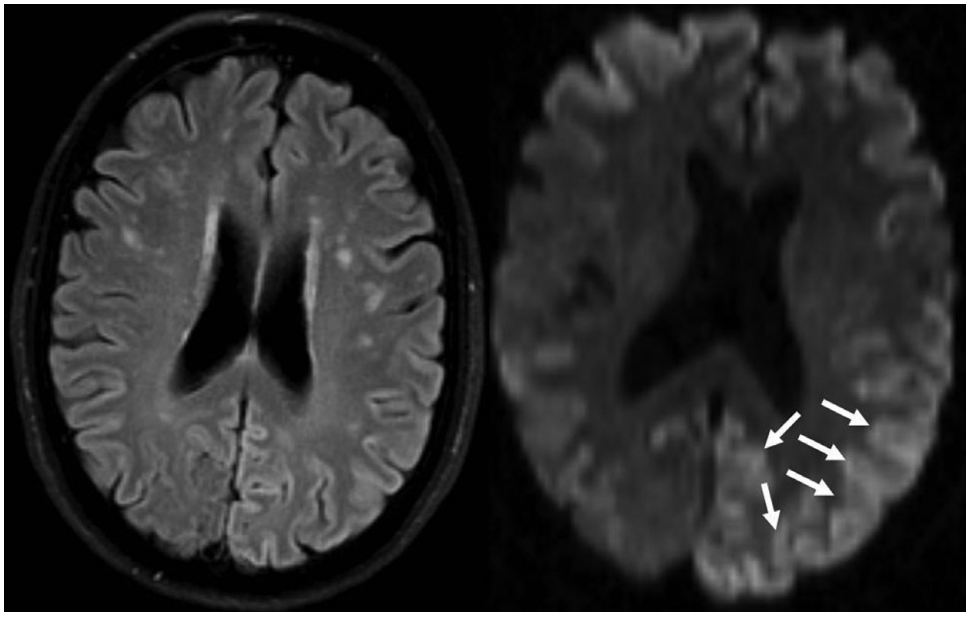

Figure 8. A 54-year-old female presenting with a cortical variant of Creutzfeldt-Jakob disease. The axial FLAIR (left) and more sensitively the DWI sequence (right) shows high signal abnormalities in the cortical gray matter of both hemispheres, more pronounced in the left parietal lobe (arrows).

such as FDG-PET and amyloid-PET for these purposes, the need for serial MRI in order to support the diagnosis is substantially decreasing. However, atrophy progression assessed by MRI is increasingly used as a safety and efficacy outcome measure in clinical trials (Frisoni *et al.*, 2010).

Conclusion

Structural MRI has become a crucial part of the diagnostic evaluation of memory clinic patients, which is reflected by current guidelines dealing with the diagnosis of dementia. Similar to CT, MRI can exclude possibly (surgically) treatable causes of dementia and also show distinct atrophy patterns and cerebrovascular changes that can support the clinical diagnosis of dementia. For these purposes, visual rating scales have been established and allow a fast, reliable and reproducible assessment. However, MRI has substantial advantages over CT and can demonstrate certain aspects of pathology associated with dementia, such as MBs as a marker of CAA associated with AD pathology and/or vascular damage. In addition, MRI is able to further characterize the amount and distribution of cerebrovascular pathology, which impacts the diagnosis, prognosis and therapeutic strategy in these patients. In some disease entities, such as prion disease, MRI has become the key diagnostic modality for a sensitive and specific diagnosis.

Despite the high value of structural MRI in the diagnostic scheme of memory clinic patients, advanced and quantitative imaging modalities, including PET and quantitative MRI techniques discussed elsewhere in this special issue, will shed further light on the dynamic field of the possibilities and challenges of neuroimaging in dementia.

Conflict of interest

None.

Acknowledgments

The author wishes to thank Professor Frederik Barkhof and Dr. Jeroen D.C. Goos for their support and critical reading of the manuscript.

References

Bastos-Leite, A. J., van Straaten, E. C., Scheltens, P., Lycklama, G. and Barkhof, F. (2004). Thalamic lesions in vascular dementia: low sensitivity of fluid-attenuated inversion recovery (FLAIR) imaging. *Stroke*, 35, 415–419.

Bouwman, F. H. *et al.* (2007). CSF biomarkers and medial temporal lobe atrophy predict dementia in mild cognitive impairment. *Neurobiology of Aging*, 28, 1070–1074.

Boxer, A. L. *et al.* (2006). Patterns of brain atrophy that differentiate corticobasal degeneration syndrome from progressive supranuclear palsy. *Archives of Neurology*, 63, 81–86.

Braak, H. and Braak, E. (1991). Neuropathological staging of Alzheimer-related changes. *Acta Neuropathology*, 82, 239–259.

Chabriat, H. *et al.* (1998). Patterns of MRI lesions in CADASIL. *Neurology*, 51, 452–457.

Cordonnier, C. and van der Flier, W. M. (2011) Brain microbleeds and Alzheimer's disease: innocent observation or key player? *Brain*, 134, 335–344.

Cordonnier, C., van der Flier, W. M., Sluimer, J. D., Leys, D., Barkhof, F. and Scheltens, F. (2006). Prevalence and severity of microbleeds in a memory clinic setting. *Neurology*, 66, 1356–1360.

Davatzikos, C., Bhatt, P., Shaw, L. M., Batmanghelich, K. N. and Trojanowski, J. Q. (2010). Prediction of MCI to AD via MRI, CSF biomarkers, and pattern classification. *Neurobiology of Aging*. Epublished ahead of print. doi:10.1016/j.neurobiolaging.2010.05.023.

DeCarli, C. S. (2006). When two are worse than one: stroke and Alzheimer's disease. *Neurology*, 67, 1326–1327.

de la Torre, J. C. (2004). Alzheimer's disease a neurodegenerative or a vascular disorder? Data, dogma, and dialects. *Lancet Neurology*, 3, 184–190.

Dubois, B. *et al.* (2007). Research criteria for the diagnosis of Alzheimer's disease: revising the NINCDS-ADRA criteria. *Lancet Neurology*, 6, 734–746.

Fazekas, F. *et al.* (1987). MR signal abnormalities at 1.5T in Alzheimer's disease and normal ageing. *AJR American Journal of Roentgenology*, 149, 351–356.

Frisoni, G. B. *et al.* (2007). The topography of grey matter involvement in early and late onset Alzheimer's disease. *Brain*, 130, 720–730.

Frisoni, G. B., Fox, N. C., Jack, C. R. Jr, Scheltens, P. and Thompson, P. M. (2010). The clinical use of structural MRI in Alzheimers disease. *Nature Review of Neurology*, 6, 67–77.

Goos, J. D. *et al.* (2009). Patients with Alzheimer disease with multiple microbleeds: relation with cerebrospinal fluid biomarkers and cognition. *Stroke*, 40, 3455–3460.

Goos, J. D. *et al.* (2010). Incidence of cerebral microbleeds: a longitudinal study in a memory clinic population. *Neurology*, 74, 1954–1960.

Gorno-Tempini, M. L. *et al.* (2011). Classification of primary progressive aphasia and its variants. *Neurology*, 76, 1006–1014.

Guermazi, A. *et al.* (2007). Neuroradiological findings in vascular dementia. *Neuroradiology*, 49, 1–22.

Hort, J. *et al.* (2010). EFNS guidelines for the diagnosis and management of Alzheimer's disease. *European Journal of Neurology*, 17, 1236–1348.

Inzitari, D. *et al.* (2009). Changes in white matter as determinant of global functional decline in older independent outpatients: three year follow-up of LADIS (leukariosis and disability) study cohort. *BMJ*, 339, 2477.

Jack, C. R. Jr. *et al.* (1998). Rate of medial temporal lobe atrophy in typical aging and Alzheimer's disease. *Neurology*, 51, 993–999.

Jones, B. F. *et al.* (2006). Differential regional atrophy of the cingulate gyrus in Alzheimer disease: a volumetric MRI study. *Cerebral Cortex*, 16, 1701–1708.

Johnston, S. C. *et al.* (2004). Cognitive impairment and decline are associated with carotid artery disease in patients without clinically evident cerbrovascular disease. *Annals of Internal Medicine*, 140, 237–247.

Kalaria, R. N. and Ballard, C. (1999). Overlap between pathology of Alzheimer's disease and vascular dementia. *Alzheimer Disease and Associated Disorders*, 13 (Suppl. 3), S115–S123.

Karas, G. *et al.* (2007). Precuneus atrophy in early-onset Alzheimer's disease: a morphometric structural MRI study. *Neuroradiology*, 49, 967–976.

Kirsch, W. *et al.* (2009). Serial susceptibility weighted MRI measures brain iron and microbleeds in dementia. *Journal of Alzheimer's Disease*, 17, 599–609.

Likeman, M. *et al.* (2005). Visual assessment of atrophy on magnetic resonance imaging in the diagnosis of pathologically confirmed young-onset dementias. *Archives of Neurology*, 62, 1410–1415.

Linn, J. *et al.* (2010). Prevalence of superficial siderosis in patients with cerebral amyloid angiopathy. *Neurology*, 74, 1346–1350.

McKhann, G., Drachman, D., Folstein, M., Katzman, R., Price, D. and Stadlan, E. M. (1984). Clinical diagnosis of Alzheimer's disease: a report of the NINCDS-ADRDA work group under the auspices of the Department of Health and Human Services Task Force on Alzheimer's Disease. *Neurology*, 34, 939–944.

Neary, D. *et al.* (1998). Fronto-temporal lobar degeneration: a consensus on clinical diagnostic criteria. *Neurology*, 51, 1546–1554.

Oba, H. *et al.* (2005). New and reliable MRI diagnosis for progressive supranuclear palsy. *Neurology*, 64, 2050–2055.

Pasquier, F. *et al.* (1996) Inter- and intraobserver reproducibility of cerebral atrophy assessment on MRI scan with hemispheric infarcts. *European Neurology*, 36, 268–272.

Poels, M. M. *et al.* (2011). Incidence of cerebral microbleeds in the general population: the Rotterdam Scan Study. *Stroke* 42, 656–661.

Pohjasvaara, T., Mätyla, R., Ylikoski, R., Kaste, M. and Erkinjunti, T. (2000). Comparison of different clinical criteria (DSM-III, ADDTC, ICD-10, NINDS-AIREN, DSM-IV) for the diagnosis of vascular dementia. National Institute of Neurological disorders and Stroke-Association Internationale pour la recherché at l'enseignement en neurosciences. *Stroke*, 31, 2952–2957.

Riidha, B. H. *et al.* (2006). Tracking atrophy in familial Alzheimer's disease: a serial MRI study. *Lancet Neurology*, 5, 828–834.

Román, C.G. *et al.* (1993). Vascular dementia: diagnostic criteria for research studies. Report of the NINDS-AIREN international workshop. *Neurology*, 43, 250–260.

Rosen, H. J. *et al.* (2002). Patterns of brain atrophy in frontotemporal dementia and semantic dementia. *Neurology*, 58, 198–208.

Scheltens, P. *et al.* (1992). Atrophy of the medial temporal lobe on MRI in probable Alzheimer's disease and normal ageing brain: diagnostic value and neuropsychological correlates. *Journal of Neurology Neurosurgery and Psychiatry*, 55, 967–972.

Scheltens, P. *et al.* (1998). White matter changes on CT and MRI: an overview of visual rating scales. *Eur Neurol*, 39, 80–89.

Scheltens, P., Fox, N., Barkhof, F. and De Carli, C. (2002). Structural magnetic resonance imaging in the practical assessment of dementia: beyond exclusion. *Lancet Neurology*, 1, 13–21.

Shiga, Y. *et al.* (2004). Diffusion-weighted MRI abnormalities as an early diagnostic marker for Creutzfeldt-Jacob disease. *Neurology*, 63, 443–449.

Shiino, A. *et al.* (2008). Different atrophic patterns in early- and late-onset Alzheimer's disease and evaluation of clinical utility of a method of regional z-score analysis using voxel-based morphometry. *Dementia and Geriatric Cognitive Disorders*, 26, 175–186.

Tschampa, H. J., Zerr, I. and Urbach, H. (2007). Radiological assessment of Creutzfeldt-Jacob disease. *European Radiology*, 17, 1200–1211.

Tzourio, C. *et al.* (2003). Effects of blood pressure lowering with perindipril and indamide therapy on dementia and cognitive decline in patients with cerebrovascular disease. *Archives of Internal Medicine*, 163, 1069–1075.

van Straaten, E. C. W., Scheltens, P. and Barkhof, F. (2004). MRI and CT in the diagnosis of vascular dementia. *Journal of Neurology Science*, 226, 9–12.

Vernooij, M. W., Ikram, M. A., Hofman, A., Krestin, G. P., Breteler, M. M. and van der Lugt, A. (2009). Superficial siderosis in the general population. *Neurology*, 73, 202–205.

Vitali, P. *et al.* (2008). Neuroimaging in dementia. *Seminars in Neurology*, 28, 467–483.

Warmuth-Metz, M. *et al.* (2001). Measurement of the midbrain diameter on routine magnetic resonance imaging: a simple and accurate method of differentiating between Parkinson disease and progressive supranuclear palsy. *Archives of Neurology*, 58, 1076–1079.

Wattjes, M. P. *et al.* (2009). Diagnostic imaging of patients in a memory clinic: comparison of MR imaging and 64-detector row CT. *Radiology*, 253, 174–183.

Zeidler, M. *et al.* (2000). The pulvinar sign on magnetic resonance imaging in variant Creutzfeldt-Jacob disease. *Lancet*, 355, 1412–1418.